TIDES, CIRCULATION AND WATER MASSES IN MAPUTO BAY

Victor F. Saide

Department of Oceanography
GÖTEBORG 2000

GÖTEBORGS UNIVERSITET
Institutionen för geovetenskaper
Avdelningen för Oceanografi
Geovetarcentrum

TIDES, CIRCULATION AND WATER MASSES IN MAPUTO BAY

Victor F. Saide

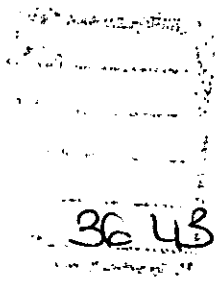

ISSN 1400-3821

B245
Projektarbete
Göteborg 2000

Postadress
Geovetarcentrum
S-405 30 Göteborg

Besöksadress
Geovetarcentrum
Guldhedsgatan 5A

Telefon
031-773 28 70

Telfax
031-773 28 88

Earth Sciences Centre
Göteborg University
S-405 30 Göteborg
SWEDEN

Tides, Circulation and Water Masses in Maputo Bay

By

Fernando Victor Martins Saide

Departamento de Física

Universidade Eduardo Mondlane

C.P. 257, Maputo, Mozambique

Thesis for *Master of Science* degree in *Physical Oceanography* at the *Gothenburg University, September 2000*

Earth Science Centre

Department of Oceanography

Box 460

SE- 405 30 Gothenburg, Sweden

Dedication

To my parents Martins Saide Mussa and Daulisa Victor

ABSTRACT

Maputo Bay is a large and relatively shallow bay in the southern part of Mozambique. It is strongly affected by tidal circulation and rich in marine life. It is important for fishing, tourism, recreation and shipping, but also as a recipient for sewage from the city of Maputo. In this thesis, hydrography, circulation and water masses in Maputo Bay are discussed on the basis of sea level, velocity, temperature and salinity observations from two sites near the entrance of the bay. Observations were made during 35 days in March-April 1993. The maximum tidal velocities exceeded 1 m/s, whereas the maximum salinity reached 35.3 on the oceanic side. The minimum salinity was approx. 33, indicating a non-negligible supply of freshwater. The temperatures varied by about 1°C on the diurnal time-scale and decreased from 26.5 °C to 24.5 °C during the period of observations. From harmonic analysis we found a purely semidiurnal tide with neap and spring tidal ranges of 0.7 and 2.5 m, respectively. The current velocity lags approx. 90-120° behind sea level. A distinct salinity pattern was seen; the lateral salinity gradients were 0.05-0.1 psu/km and the eastern side was more saline than the western. By studying salt and volume fluxes as functions of salinity, we found a net volume flux (residual circulation) of 3000 m^3/s basically outwards in the salinity interval from 34.7-34.9 and inwards from 34.9 to 35.2. The tidal fluxes were of the order 10^5 m^3/s, whereas the net circulation was just a few cm/s. The salinity data indicates that the residual circulation clockwise, with an inflow on the eastern side and an outflow on the western. During the period of observations, we found a freshwater supply of 200-300 m^3/s. The residence time for the Maputo Bay water vs the oceanic was estimated to approx. 2 weeks.

Keywords: tides, circulation, fluxes, residual currents, residence time, harmonic analysis, Mozambique, Maputo Bay

Content

1. INTRODUCTION

1.1 General introduction

The Maputo Bay in southern Mozambique is a large, semi-enclosed shallow bay which receives waste water disposal from Maputo and freshwater from several smaller rivers. The bay area is shown in Fig. 1. Tides are the main flushing mechanism (Hoguane, 1994). The bay provides food for the surrounding population and there are also well recognised, attractive sites for tourism and recreation developed around the bay. This work contains an effort to describe circulation and mixing processes in Maputo Bay on the basis of some current, tide, salinity and temperature measurements.

Already in the 50'ies, a biological research station was set upon Inhaca Island, situated on the eastern side of the Maputo Bay. From here, studies were carried out also on marine sciences, particularly on surrounding sea-grass beds and mangroves. With that, a need for better knowledge of tides and circulation processes also developed. We hope that the outcome of this study can become useful for future marine research in the bay.

Marine research in the Maputo Bay area has been concerned mainly with its marine biology and ecology (e.g. Halton, 1990; Bandeira, 1995). Studies on physical oceanography are sparse. Up to recently the deep sea region outside the bay was clearly better known; mostly because of studies on the currents in the Mozambique Channel (e.g. Saetre and da Silva,1984; Saetre, 1985; Donguy and Piton,1991). Very few efforts have actually been devoted to the circulation and hydrography of the bay itself, although it seems as if there is now an increasing interest for the physical processes as well. Lobo *et al.* (1973) were probably the first to describe the hydrography of the bay. Their report was based on observations of salinities and temperatures collected weekly at six different stations in the bay. The report offers a qualitative picture of the seasonal salinity variations in relation to freshwater runoff. Much later, in a study of oil drift, Hoguane (1994) applied a 2-D depth-averaged tidal model which produces particle tracks. In his thesis work, an extensive study of Ponta Rasa Creek on the Inhaca Island, Hoguane (1996) also discusses the circulation of Maputo Bay, particularly with respect to it influences on the water exchange within creeks.

During a regional workshop, combined with coursework on physical oceanography, Queface (1996) studied the temperature and salinity variability and Saide (1996) examined the tidal currents in the bay. Both studies were based on a data set obtained from two current meters, deployed in the northern part of Maputo Bay. The same set of raw data is used extensively in this work. By applying various methods for treatment of the observations, such as harmonic analyses of tides, currents and salinities, volume and salt conservation applied by using salinity as independent variable, etc. we aim at improving the knowledge of circulation, water exchange and mixing conditions with in the bay.

1.2 Problem statement

An increasing demand for food including other basic needs implies a substantial pressure on the national resources Mozambique. In this respect, fisheries along the coast which is 2700 km long, is very important. For a sustainable and still efficient use of the coastal resources including the management of the offshore waters, there is a clear need for a solid understanding of the physics of the coastal ocean. That includes both tides, tidal currents and winds including their effects on mixing and exchange processes. This is particularly true for the Maputo Bay where the shipping and waste-water from the highly populated city of Maputo may cause serious damage to the living resources.

Main questions, which have been raised several time before is whether there is a net circulation in Maputo Bay and how efficient the water renewal is. Which forcing mechanisms can explain water exchange and residual currents in the bay? And further, can the biological life within the bay be sustained at the present level of waste water input? Whereas some of the former questions can be partly resolved in this thesis, the later one is still an issue for the future.

1.3 The study area

Maputo Bay is a semi-enclosed more than1000 km^2 large bay located in southern-most part of Mozambique at latitude 25 55'S to 26 10'S and longitude 32 40'E to 32 55'E. It has a mean depth of about 10 m at MSL. The topography which varies substantially, including the physical dimensions are shown in Fig. 1. With a wide mouth open to the north, Maputo Bay is bounded on the eastern side by the Portuguese and Inhaca Island and the Machangulo Peninsula. This natural barrier protects the bay from the open ocean wave influence. On its western side is Maputo city and its surroundings. In the south is Matutuine, a sparsely populated area.

In most areas, the water depth is less than 10 m, whereas in some channels and at the entrance it exceeds 20 m. There are several sand banks and channels basically in the north-south direction. A narrow strait on the eastern side, south of Inhaca Island (Ponta Torres Strait), allows for a very restricted water exchange with the open sea. The Maputo Bay features vast intertidal flats. About 30% of the bay area dries out at low water spring (see Fig. 3). The largest intertidal flats are found in southern part of the bay.

As a part of the great Mesozoic Cenozoic sedimentation zone the drainage basin for the Maputo Bay area consists of rocky sandstone and dark sand areas, whereas the plains are deeply eroded as a result of Pleistocene and post-Pleistocene transgression-regressions of the sea level (dos Muchangos, 1994). On the western and southwestern side of the bay, strong erosion and sedimentation characterise the shaping of the coast including the mudflats and the intertidal areas have become enlarged in the late years (dos Muchangos, 1994).

Grass and trees of savanna type characterise the vegetation of the areas surrounding Maputo Bay. There are also swamps in some places. The littoral vegetation consists of dense coastal forest and mangroves including open forests of miombo. Seagrass beds are common (cf Bandeira,1995). Some of the southernmost coral reefs in the world are found on the eastern side of the bay near Inhaca Island. The reefs also feature a very diverse fish fauna.

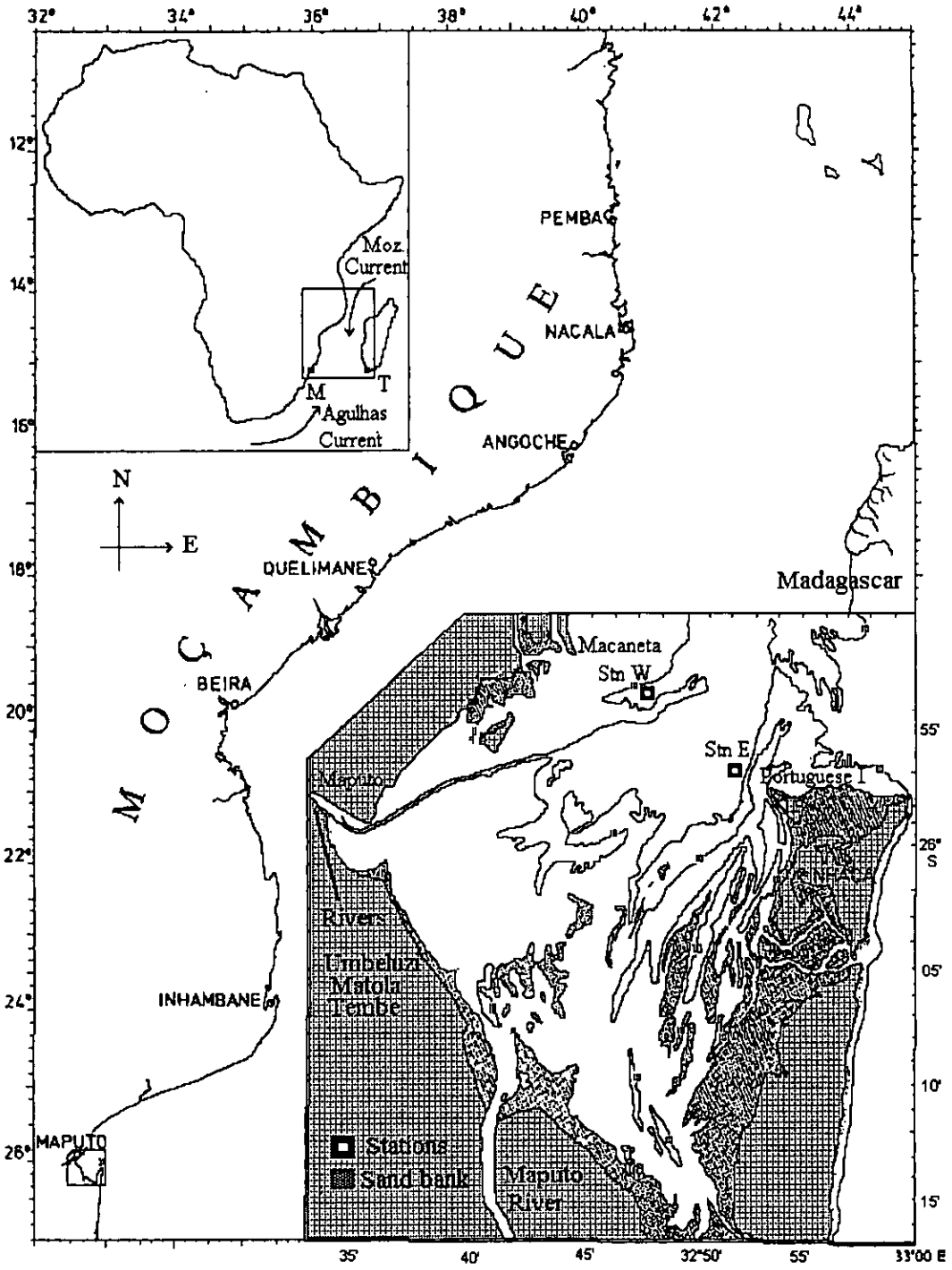

Fig 1 *Maputo bay showing the bathymetry and mooring sites including the coastline Mozambique, Agulhas Current and Mozambique Current; M-Maputo, T-Tulear*

The Maputo Bay area is near to the southern border of the tropical climate zone. It has two seasons: the warm rainy and the cold dry season. The rain season normally occurs from October to March while the dry season occurs between April and September. The yearly precipitation is 780 mm with maximum in December and January, during the southern

summer. The daily mean air temperature varies from ca. 20 °C in southern winter to 25 °C during summer. Mean monthly values of temperature and precipitation are shown in Fig. 2.

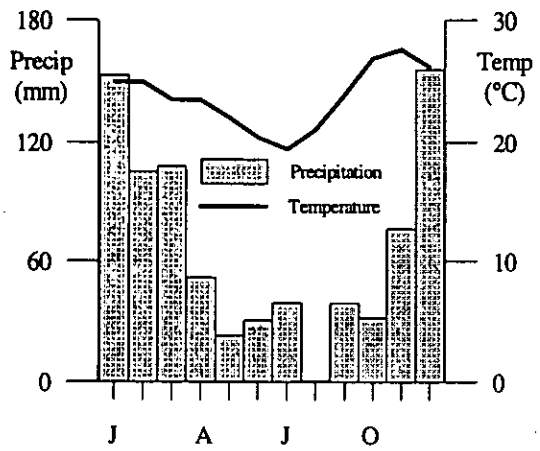

Fig. 1 *Monthly average temperatures and precipitation (1960-75; Stn Matutuine):*

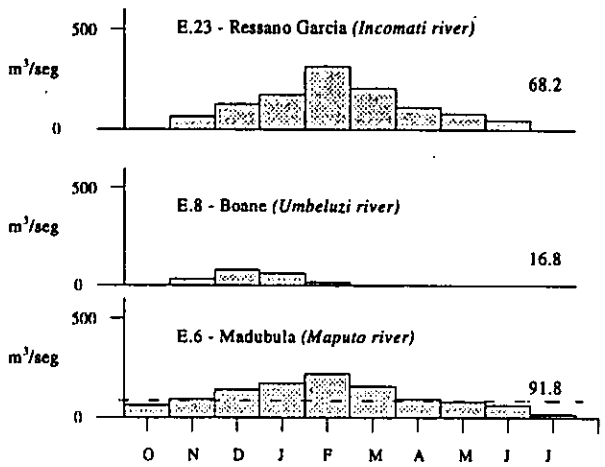

Fig. 2 *River runoff at gauges upstream in Incomati, Umbeluzi and Maputo rivers. (1960-1975; from MINED, 1986)*

The winds are dominated by the SE trade wind with mean wind forces of 3-4 m/s only (Saetre, 1985; citing US Naval Oceanographic Office). It seems as if the winds within the Maputo Bay are stronger than those observed over land and weaker than those observed in the open sea (Hoguane, 1996). Moreover, the winds over the bay are influenced by a diurnal sea-breeze which strengthen the trade winds considerably, particularly in the afternoons (dos Muchangos, 1994). Occasionally hurricanes appear. At a regional level the wind system seems to be important for the major warm currents in the Mozambique Channel. For instance, although far away from Maputo, the NE monsoon is suggested to strengthen the southward flow through the Mozambique Channel during the southern summer (Donguy and Piton, 1991), implying higher temperatures and salinities than otherwise expected.

Five rivers drain into the bay, the Incomati river in the northern end, Umbeluzi, Tembe and Matola on the western side and Maputo river in south-west. The rivers Umbeluzi, Tembe and Matola join in the Maputo harbour (Fig.1). Fig. 2 shows data from observations upstream in some of the significant rivers. The highest flows are recorded in Incomati and Maputo river, and the yearly mean freshwater supply to the bay is 200-300 m^3/s (see also Saetre and da Silva, 1984). Maximum discharge occurs from January to March while August and September are practically dry. Fig. 7 and Table 3 also indicate long-term seasonal runoff from the three main rivers.

Following Lobo *et al.* (1973) it seems to be distinct a difference in temperatures and salinities between the western and the eastern side of the Maputo Bay. On the eastern, oceanic side there is a nearly constant salinity of about 35 throughout the total year, while the salinity on the western side is definitely more variable, as influenced by river discharge and rainfall. The water temperatures in the bay range from 17 °C during the southern winter to 27 °C during the summer. Thus the annual range within the bay is larger than that of the open ocean where it reaches 3-4 °C, only.

According to Hoguane (1996) and the Admirality tide tables, the tides in Maputo Bay are semi-diurnal, with a spring tidal range of about 3 m. The range in Maputo harbour which offers a tide gauge for navigation, is slightly less than that at Baixos do Inhaca outside the bay. Further, the high tide in Maputo is delayed by approx. 30 minutes in comparison with the high tide at the entrance of the bay.

As mentioned, tourism and recreation activities are frequent along the shorelines of the bay. Fishing, including collection of marine invertebrates dominate the human utilisation. Some species like sea cucumbers, *Holothuria scabra* are collected in the sea grass beds and on nearby sand banks (Bandeira,1995). Industrial and domestic sewage, including harbour activities are probably the main sources of pollution in the bay although oil spill from accidents in cargo handling is also a common threat. All these activities are likely to exert an influence on the water quality of the bay, its flora and fauna. Pollution effects have been illustrated by large quantities of opportunistic algae, such as *Ulva* and *Enteromorpha* (Bandeira, 1995). There is evidence of mangrove deforestation even within the city limits, which may increase erosion and decrease water visibility in the bay area.

1.4 The Mozambique Current

Due to the tides and the related tidal currents there is a continuous exchange of water between the Maputo Bay and the open ocean. The efficiency of this exchange also depends on the warm Mozambique Current which flows southwards through the Mozambique Channel. With a steady south-ward flow, most of the water that leaves the Maputo Bay during ebb will be brought away from the area by the current. If weak, however or involved in local gyres, the same water which left the bay during ebb will enter again during the next flood. In such case the exchange is small. The Mozambique Current is usually considered as a part of the anticyclonic subtropical gyre consisting of South Equatorial Current, the Agulhas Current system and the eastward flow north of subtropical convergence zone (Saetre and da Silva, 1984). The circulation in Mozambique Channel is characterised by several cyclonic and anticyclonic vortices. The early ideas by Soares (1975) implying that the Mozambique Current does not show the pattern of well defined continuous western boundary current still seem to hold. The seasonal fluctuations within the Mozambique Current were discussed in detail by Saetre and da Silva (1984). Lutjeharms and Grundling (1989) and Donguy and Piton (1991) included discussions also on inter-annual variations. By referring to the meridional transport through the northern part of the Mozambique Channel they observed maximum current velocitites during the NE monsoon from October to January.

From November to March, during the southern summer, the sea level is high in the southern part of the Mozambique Channel including the Maputo Bay but initially it is even higher on the Madagascar side of the channel, at Tulear indicating a strengthening of the southward flow during southern summer (Donguy and Piton, 1991). The Mozambique Current is about 3 °C warmer during summer (Donguy and Piton, 1991), partly because of seasonal high radiation but also, reasonably because the transport from the tropics occurs faster. The salinities average 35, with a weak seasonal variation from 34.8 in summer to 35.3 in winter (Saetre and da Silva, 1984). During summer the temperature in the current may reach 25-26 °C while during winter, typical values seems to be in the range from 22-24 °C.

1.5 Coastal dynamics and mixing processes

The tide plays a major role for the dynamics of most coastal embayments and estuaries. It provides the necessary energy for mixing of waters with different densities and for transport of sediments and other constituents (Heath, 1981). However, also winds and freshwater

supply may contribute to the dynamics. If the tides are weak, such factors may even dominate the circulation. There are a lots of studies on these subjects. Some few papers are mentioned below.

Uncles and Jordan (1979) estimated long-term net fluxes of water and salt at two stations in the Severn estuary. They found that the residual flow was the dominant mechanism for transport of salt towards the ocean, balanced by a salt transport into the estuary caused by tidal pumping. Vertical shear was of secondary importance in the balance. The freshwater supply determined the long term cross-sectional averaged residual transport.

Heath (1981) defined a mixing parameter from the relation between the loss of tidal energy and tidal elevation harmonic constants, involving the freshwater inflows. He pointed out that frictional dissipation of tidal energy within a coastal embayment leads to an increasing delay in the time of high tide land-ward from the entrance. Stigebrandt (1980) arrived at similar conclusions from studies of different estuarine systems with constrictions. He also established a relationship between phase lag, tidal amplitudes and the loss of tidal energy.

Robinson *et al.* (1983) studied and modeled the salinity variations in an English tidal lagoon, The Fleet for different freshwater supply. The salinity distribution was described in relation to both circulation and mixing processes in the lagoon. Robinson *et al.* compared the tidally driven salt diffusion along the mean gradient with advection of salt by the mean residual flow and determined the flushing time in different parts of The Fleet. They also discussed the importance of the river discharge in relation to the tidal flushing.

Swift and Brown (1983) estimated the area-averaged bottom stress in four channel segments of the Great Bay Estuary. From current and sea level measurements at tidal frequencies they calculated and compared acceleration and pressure gradient terms in the equation of motion. They found large values for both stress and energy dissipation in the seaward portion of the estuary. A decrease in dissipation at most inland sites allowed them to characterize the estuary by two different regimes: one highly dissipative, more progressive tidal wave regime, seaward and one less dissipative, standing wave regime land-ward.

Prego and Fraga (1992) presented a simple model for calculating residual flows in an estuary considering salinity as a tracer. Applying their model to the estuary of Rio Vigo they found that when the freshwater flow increased during summer, the vertical mixing decreased implying less exchange of deeper water. Despite weak river discharge in Maputo Bay it may be interesting to estimate at which strength the mixing occurs.

Arulanantan *et al.* (1995) examined the influence of precipitation, freshwater supply and evaporation on the seasonal salinity cycle in the Puttalam Lagoon using both recent and older hydrographic data. They observed a 10 psu increase in the average salinity of the lagoon over a thirty year period. Reduced river discharge was found to be the main reason. Rapidly decreasing salinities during rainy season and increasing salinities during the dry season could be explained from variations in evaporation and precipitation over the lagoon.

Focusing on the specific contribution of tidal currents to dispersion and flushing of estuaries, Geyer and Signell (1992) showed that the tidal dispersion is likely to be the dominant agent for horizontal mixing in regions of abrupt topographic variation. They also provided information on the processes controlling the distributions of waterborne biota, nutrients, sediment and contaminants.

Studying estuaries of constant width and depth Ianniello (1977;1981) derived two-dimensional analytic solutions for the Eulerian and Lagrangian residual currents by a perturbation method. Iannello considered non-linear interactions of the first order tides and showed that the previous studies based on boundary layer approximation were not valid for realistic depths and magnitudes of the eddy viscosity coefficient. The boundary layer analysis simply assumes that the first order flow is frictionless except in a thin layer near the bottom. Nonlinearly induced residual currents are significant only if they are comparable with other steady currents driven by river discharge or density gradients. They occur only in partially stratified waters where currents are relatively strong and the density gradient is weak and two-layer circulation is the main feature.

Some references to studies of coastal bays affected by tides have been mentioned above. In fact there are several more within the field; Dyer and Taylor (1973), Hughes and Rattray (1979), Brown and Trask (1979), Oey (1984), Wattayakorn *et al.* (1990), Jay and Smith

(1990a; 1990b), Officer and Kester (1991), Medeiros and Kjerfve 1993, Wong (1994) and Rydberg *et al.* (1996) to mention another few. Last, but not least, we should mention a paper by Walin (1977) who, followed by several others (e.g. Andersson and Rydberg, 1993), introduced a description of estuarine circulation which was based on salinity as independent variable. In a forthcoming effort to balance the salt and volume flux we will use a similar approach.

2. MATERIALS AND METHODS

2.1 Instruments and data collection

The data used in this study were collected by the Instituto de Investigação Pesqueira in Maputo in co-operation with the Institute of Marine Research, Bergen, Norway. Two current meters were deployed from 8 April to 13 May 1993 at two different stations near to the northern entrance of the Maputo Bay, Stn E on the eastern side near Portuguese Island and Stn W further towards west. The locations are shown in Fig. 1. The moorings consisted of one current meter (Aanderaa, RCM-7) each. On Stn E, a pressure gauge was placed on the bottom. The depths at the moorings were 21 and 17 m for Stn E and Stn W respectively. The current meters were operating at 10 m depth, sampling current speed and direction, salinity and temperature at 10-min intervals. The tide gauge also sampled every 10 minutes. Instrument specifications are given in Table 5.

Meteorological data were obtained from the Instituto Nacional de Meteorologia (INAM). River discharge for the rivers entering Maputo Bay were obtained from Direcção Nacional de Águas (DNA). Bathymetric maps of the study area were provided by Instituto Nacional de Hidrografia e Navegação (INAHINA).

2.2 The hypsographic curve

By means of a bathymetric map of the bay and a mechanical planimeter, some hypsographic curves were constructed. Surface area and volume of the bay as a function of depth are shown in Fig. 3. The outer border for the calculation is shown in Fig. 1. The topography of the cross section at the border, i.e. the entrance of the bay, is shown in Fig. 4. The volume at high water spring (HWS) is 9.1 km^3 and at low water spring (LWS) 5.6 km^3. Thus, the tidal prism is 3,5 km^3 during spring. During neap the prism is 1.2 km^3. However the topography is not well

mapped, particularly not in the southern parts, and the figures on tidal prism may therefore be a bit uncertain.

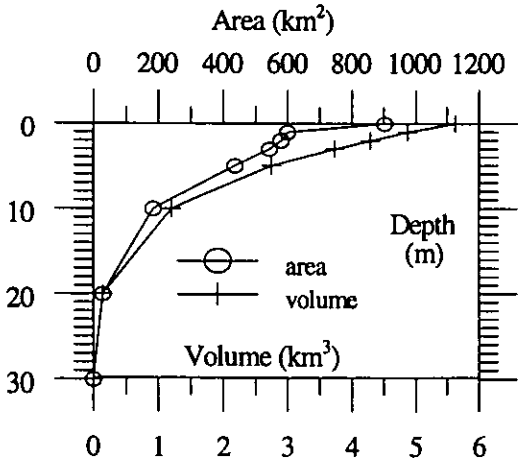

Fig. 3 *Hypsograhic curve of Maputo Bay at low water. Area (∅) and volume (+).*

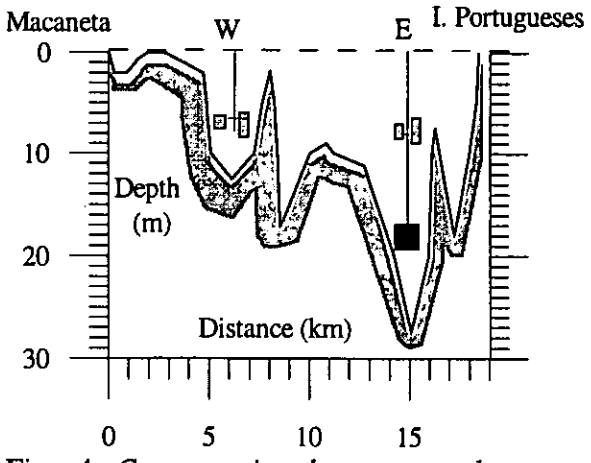

Fig. 4 *Cross-sectional area at the entrance of Maputo Bay showing the moorings.*

3. THEORY

3.1 The basics of tides

Tides and the resulting circulation and mixing are prominent phenomena occurring in most coastal estuaries and embayments. With tides we mean the alternate rise and fall of the sea level basically with 12 or 24 h periods. It is a consequence of the convergence or divergence of water currents due to the simultaneous action of the Moon's, Sun's and Earth's gravitational forces and the apparent revolution about one another (Pond and Pickard, 1983).

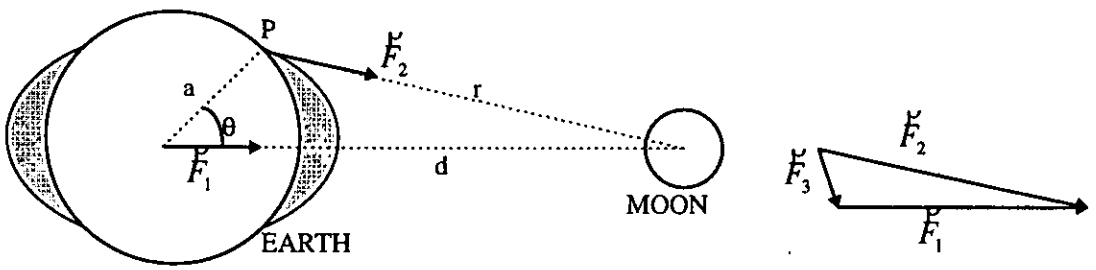

Fig. 5 *The derivation of tide generating forces from Newton law of gravitation, d-distance from the centre of Moon to the Earth centre, r distance from the centre of the Moon to the point P on the surface of the Earth, a- the Earth radius, F_1 and F_2 gravitational forces acting on the Earth centre and point P respectively*

The forcing of tides was initially studied by Newton. Applying his laws of dynamics including gravitational attraction between the Earth and Moon Sun system we derive the tide generating forces as follows from the Fig. 5. It is expressed by

$$F = \frac{3}{2}\frac{M}{E}\left(\frac{a}{d}\right)^3 g\cos 2\theta .$$

where *M(S)* is the mass of the Moon (Sun), *E* is the mass of the Earth, *a* is the Earth radius, *d* is the distance from the centers of the Earth and Moon (Sun) and θ is the angle between the lines connecting the center of the Earth and Moon (Sun) and the radius vector from the center of the Earth and point P.

The dynamic theory for tides has been successively refined by other scientists. For the description of the development of the theory, including the prediction of tides; see e.g. Franco (1980), Pond and Pickard (1983) or Bowden (1987).

Hendershott (1977) presented a summary of the theoretical view of ocean tides and described them from wave point of view putting emphasis on the dynamic importance of the ocean. Assuming a spherical Earth surface he expressed the equilibrium tide ζ through harmonic decomposition of spatial and time varying tidal potential over the gravitational acceleration in order to distinguish between long periodic, diurnal and semi-diurnal tides. Thus

$$\zeta(\phi,\theta,t) = U(\phi,\theta,t)/g = \sum_{m=0,1,2} (A_2^m \cos(m\phi) + B_2^m \sin(m\phi))P_2^m ,$$

where $U(\phi,\theta,t)$, g are the horizontal component of tidal potential Γ and gravitational constant , ϕ,θ are longitude and latitude, P_2^m the associated Legendre functions expressed by latitude instead of the colatitude $\pi/2-\theta$ (Hendershott, 1981)

$$P_2^0 = \frac{1}{3}(3\sin^2\theta - 1), \quad P_2^1 = 3\cos\theta\sin\theta, \quad P_2^2 = 3\cos^2\theta,$$

A_2^m, B_2^m are time dependent functions, also related to the amplitudes M_i and the sets of Doodson numbers $N_j^{(i)}$. Combining the first Doodson numbers 0, 1 and 2 with secular arguments $S_i(t)$ we obtain respectively long period, diurnal and semi-diurnal types.

3.2 Tidal prediction and harmonic analysis

Tidal computation for the prediction of tides was developed independent of the dynamic theory. Predictions are carried out on the basis of set of frequencies determined by the relevant astronomical factors, such as the rotation of the Earth on its axis, the Moon's revolution

around the Earth, the Earth's annual revolution around the Sun and the declination and right ascension effects from Sun and Moon ecliptics (see Doodson, 1923). A time series of sea level measurements is then analysed with reference to these frequencies.

A straightforward practical approach for tidal analysis is harmonic analysis whereby each constituent is represented by a sine curve and its amplitude contributes to a certain extent to the total amplitude of the tide. We experience different behavior of the tide at different places in the ocean. This is due to the continents which obstruct the forced "tidal wave" to move freely with the celestial bodies. A prediction of tides at particular location for a particular period of a time can be obtained from harmonic analysis of a sea level curve at this point (e.g. fitting the observations to a sum of sine curves). The predicted curve is a complex harmonic composed by several simple harmonics of different periods, phases and amplitudes.

As a mathematical tool, the harmonic analysis is based on the least squares method where differences of the phase variations of the constituents results in the difference of their angular frequencies (see Franco, 1980; Cederlöf, 1998). If z_k is an observable of a vector of N observations of a certain parameter such as sea level, salinity or velocity at a constant sampling interval $)t$ as a results of the combined effect of the harmonic interactions of different frequencies T_i we are able to extract their contribution a_i in the amplitude of variation of this parameter. Thus, we can represent z_n as a combination of I harmonic functions to $._k$, Fourier series where the best fit is obtained when

$$\sum(z_k - \varsigma_k)^2 = \text{min., i.e. } z_k \approx \zeta_k$$

Basically the method consists if fitting the curve through the set of harmonics and solving the system of a set of equation by least square method approach. Since the fitting curve is expressed by

$$\zeta(t) = \sum_{i=1}^{I} a_i \cos(\omega_i t - \varphi_i),$$

we put the left member term equal to z_k so that we obtain easily a set of equation $Ax=b$ with following solution for amplitude and phase lag respectively

$a_i = \sqrt{(a_i \cos\varphi_i)^2 + (a_i \sin\varphi_i)^2}$ and phase lag $\varphi_i = a\tan(\frac{a_i \sin\varphi_i}{a_i \cos\varphi_i})$ or the time lag

$$\tau_i = \frac{\varphi_i}{\omega_i}$$

However, for prediction purpose we consider also some factor, such as nodefactor and epoch.

A simple way of classifying tides is by the form number F, expressed as the ratio between the amplitudes of the diurnal harmonic constituents K_1+O_1 and that of the semidiurnal M_2+S_2 . F is shown in the Table beside.

Form number F	*Type of tides*
F # 0.25	semidiurnal
0.25 # F < 1.5	mixed, mainly semidiurnal
1.5 # F <3.0	mixed, mainly diurnal
F ∃ 3.0	diurnal

Table. *Classification of tides, following Pond and Pickard (1983).*

3.3 Equilibrium Theory

The equilibrium theory considers the immediate response of an ocean to the tide-generating forces, assuming that homogenous water of uniform depth covers the whole Earth and can respond instantaneously to the changing forces (see e.g. Bowden,1983). Since the tide-generating force is in balance with horizontal pressure gradient the water elevation corresponds to the equi-potential surface and a small change in the tide-generating forces implies a change in the shape of this surface. Assuming that the elevation is proportional to the potential of the tide generating forces, maximum elevation occurs when the Sun and the Moon are aligned with the Earth, at the point immediately below the Moon and on the opposite side of the Earth away from the Moon. The minimum elevation occurs as a fortnightly inequality, when the Sun and Moon are at right angles. However, the disparities between observed and calculated amplitudes and phases of equilibrium tides arise from other effects besides the astronomic like ocean self-attraction , tidal solid Earth deformation and thermal and atmospheric effects.

3.4 Dynamic Theory

In the dynamic theory, we assume that the tide-producing forces of the Moon and the Sun are generating long gravity waves of tidal frequencies in the real ocean such that the tides at a given place in ocean appear as result of superposition of all kinds of waves of tidal induced sea level variations; i.e., waves of approximate wavelength. This was first suggested by Laplace. The tides are long waves as their wavelengths are larger than ocean depth. Other assumptions are also included, such as hydrostatic pressure at any depth, no vertical acceleration, incompressible fluid and a steady state motion. Tidal motions in estuaries and embayments are generally caused by ocean tides at their entrances and not directly by tide

generating forces of Moon and Sun (Officer,1983). This is because the theoretical water elevation at a certain place does not agree with the practical result.

4. RAW DATA TREATMENT

4.1 Meteorological data

A set of long-term mean monthly meteorological data; air temperature, precipitation, evaporation, humidity, air pressure, wind speed and wind direction is summarised in Table 2. The data, from 1951-90, offers an overview of the meteorology of Maputo Bay area. Another set of similar data, which includes the period of observations (March-April 1993) presents monthly values for the year of 1993 and daily average values for the period itself. Monthly data on long term precipitation and runoff from the main rivers discharging into Maputo Bay was also included. All these data are shown in Figs 7 a-d and Figs 8 a-b.

4.2 Sea level and current meter data

The readout from the current meters and the tide gauge was carried out by use of instrument specific software. Calculation into engineering units and recalculation of total pressure observed by the tide gauge to sea level variations were made with help of programs available at the Instituto de Investigação Pesqueira, Maputo. Further we determined the trends of water elevation. The data on sea level variations are shown in Figs 9 a-b.

From the current meter data, we determined main flow directions; for Stn E we found outflow for 32° and inflow for 225°. For Stn W the corresponding directions were 51°(245°). For the forthcoming calculations of volume and salt fluxes, we determined velocity components along the main axes (cross-section velocities). Velocity and direction data are shown in Fig. 10 together with results from harmonic analysis (see Section 4.4). Temperature and salinity data from both stations are shown in Figs 11 a-b and Figs 12 a-b, respectively.

4.3 Volume, heat and salt fluxes

Simultaneous salinity and cross-section velocities (see Section 4.2) were used to calculate the volume flux across the bay entrance, M as function of salinity, S. Following Walin (1977), $M(S)$ is defined as the flux of water with salinities less than S. $M(S)$ was obtained by integrating the flow function $m(S)$, such that

$$M(S) = \int_0^S m(S)dS$$

where $m(S)$ is the flux of water within the salinity interval from S to $S+ds$. Correspondingly, the flux of salt is calculated according to the expression:

$$M_s(S) = \int_0^S m(S)SdS$$

where $M_s(S)$ stand for flux of salt for salinity less than S.

In order to determine instantaneous volume and salt fluxes across the entrance, one possibility is to find representative cross-section areas for each of the two current meters. This was not quite easy because of the strongly varying depths and the position of Stn W which was placed in a channel, which probably influenced its representativity. Thus, we averaged the cross-section velocities between the two stations as well as the salinities and temperatures, and carried out the calculations of for the whole cross-section, such that $m(S)=v(S)a(S)$; where the calculation of $m(S)$ was carried out for salinity intervals of $\Delta S=0.1$ psu. After that, an integration over salinity intervals was carried out in order to obtain $M(S)$ and $M_s(S)$. In addition, we tuned the outgoing velocities in relation to the ingoing on Stn W, such that we obtained zero salt flux for the whole observation period. The reason for tuning was that we found that the outflow on Stn W was underestimated because of the position of the current meter near to a reef just inside of the mooring. The reason for using salt conservation instead of mass (volume) in the tuning process may seem obscure, particularly as the salinity shows a decreasing trend during the later part of the study. However, we will return to this issue in the result section.

The instantaneous heat flux, H_T was calculated from the equation $H_T(t)=\rho c_p vA(t)T(t)$, where, T is the temperature, ρ the density, c_p the specific heat and A the cross-section area. By integration, over a long enough period, we can obtain the long term net flux $M_T(t)$ into or out of the bay;

$M_T(\tau) = \frac{\rho c}{\tau}\int_0^\tau vATdt$. $M_T(\tau)$ was determined for the whole period.

Volume and salt fluxes are shown in Figs 14 a-d whereas the heat flux is shown in Fig. 15.

4.4 Harmonic Analysis

All data sets, sea levels as well as velocity, salinity and temperature measurement were subject to harmonic analysis using a program developed in Matlab by Cederlöf (1998). The program identifies a maximum of 14 tidal constituents, their amplitudes and phases. Thereby it uses the position, start-time, interval of observations and number of constituents to give the amplitude

and phase lag for each constituent in relation to UTC (GMT). Results from the harmonic analysis are shown in Figs 9-12, in Table 6 (beside Fig. 9) and in Table 7-10.

4. 5 Spectral analysis and filtering

To describe the relationship between salinities, temperatures, velocities and sea level, some spectral analysis was also performed. This includes the determination of the cross correlation, coherence and density spectrum including a phase lag function by use of a Fast Fourier Transform (FFT) method which is built into an interpreter. In this case 12 degrees of freedom were used with 136 (816) elements for each time sample.

Furthermore, the data set from the two current meters were low-pass filtered. Generally, a filter multiply all amplitudes by zero for all frequency bands not of interest and by one the desired frequency band where the Jumpfunction in frequency field (low-pass) is solved through a filter $sin(x)/x$ in a time interval Δt . Considering a finite unfiltered series of N elements x_n, with a discrete time interval $\in t$ we express a numeric filter by

$$y_n = \sum_{k=-N}^{N} c_k x_{n-k}$$

where y_n is the filtered series and c_k is the filtering coefficient, determined from the Nyquist-frequency $f_n = \frac{1}{2\Delta t}$. Our desired frequency f_c follows

$$c_k = \frac{\sin(\pi f_c k)}{\pi f_c k}, \quad c_0 = \frac{f_c}{f_n}$$

In this study we used a cosine Lancsos filter and 121 points per sample. Some results from the spectral analysis are shown in Fig. 16 and 17.

5.1 Hydrometeorological data

Long term data on monthly river discharge and precipitation are shown in Figs 7 a-b. Maximum discharge occurs in February. However, two peaks occur for Incomati river (Stn Magude) during the hydrological year of 1992-93 (October to September). Daily average values of air temperature, wind speed and wind direction including precipitation and the discharge of Incomati during April 1993 are shown in Figs 8 a-d. On average the air temperature and the discharge are decreasing during April. This feature is related to the seasonal variations of these parameter, because this is the period with a transition towards a drier and colder season. The mean winds are weak but some days of stronger winds occur during the first and last days of the observations. Southerly or northwesterly winds are the most common; approximately 40%(30%) of the whole period of observations. This figure is consistent with the general pattern of winds throughout the year, shown in Table 2.

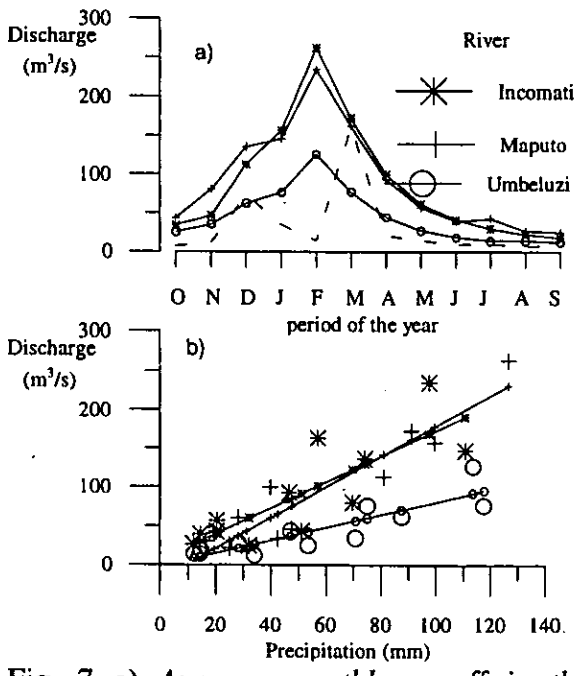

Fig. 7 a) *Average monthly runoff in the rivers Incomati, Maputo and Umbeluzi for the period 1951-90 and for Incomati from October 1992 to September 1993 (----);* b) *Relation between runoff and precipitation on 1951-90 data (see also table 2, annex)*

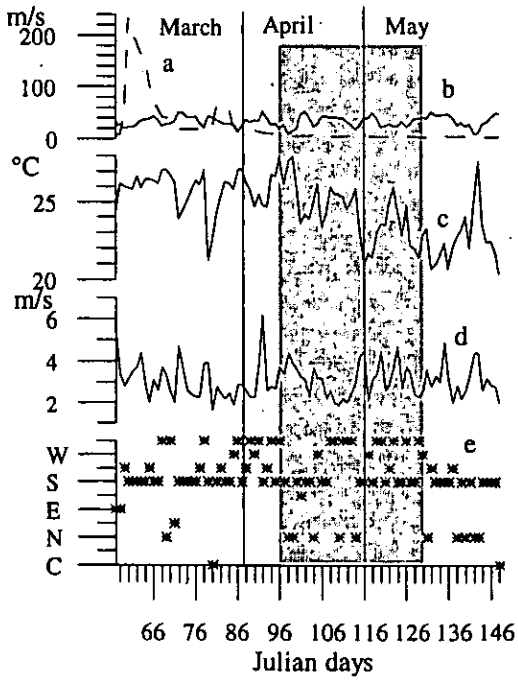

Fig. 8 *Daily average data: a- Incomati river runoff, b- precipitation, c- air temperature, d- wind speed and e- direction from 1993. The period of observations is shaded.*

5.2. Observations and tidal analysis

Sea level

The computed and residual records of the sea level as determined from harmonic analysis are shown in Fig. 9 together with the original record. Amplitudes and relative phase lags for the constituents are indicated in Table 6. The spring and neap tidal range $2(M_2+S_2)$ and $2(M_2-S_2)$ respectively are 2.52 m and 0.72 m, with a maximum range at spring of about 3 m, similar to the Admirality Tables. The observations started during spring tide and ended up at neap. A form factor of 0.06 shows that the tides in Maputo Bay are purely semi-diurnal. Maximum spring tide occurs 34 h after a passage of the full or new Moon (see Table 7, annex).

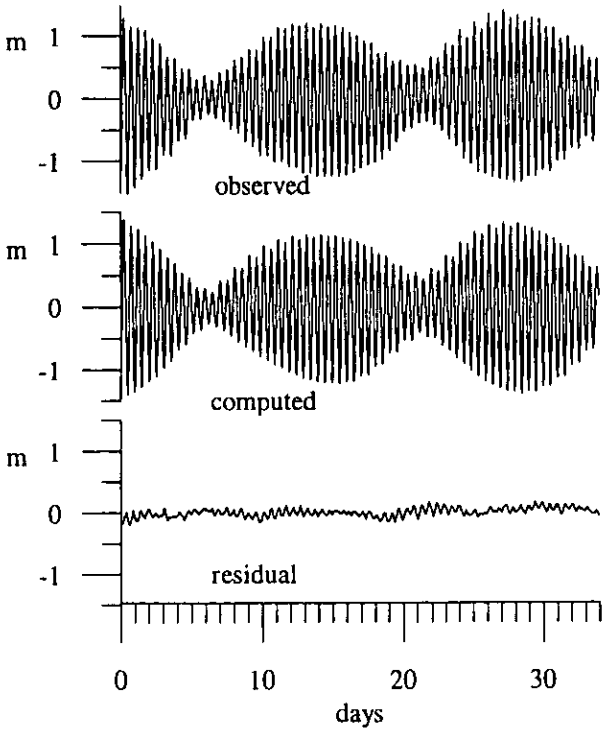

Table 6: *Result of harmic analysis*

Const *Symbol*	Amplitude *(m)*	Phase lag *(°)*
M_2	0.81	87.0
K_1	0.05	185.2
S_2	0.45	126.6
O_1	0.03	6.1
K_2	0.11	118.2
P_1	0.02	163.2
N_2	0.14	65.8
M_f	0.06	38.2
$2SM_2$	0.02	289.9
M_4	0.01	11.2
MS_4	0.003	57.9
S_4	0.003	61.6
M_6	0.007	245.3
$2MS_6$	0.008	271.9

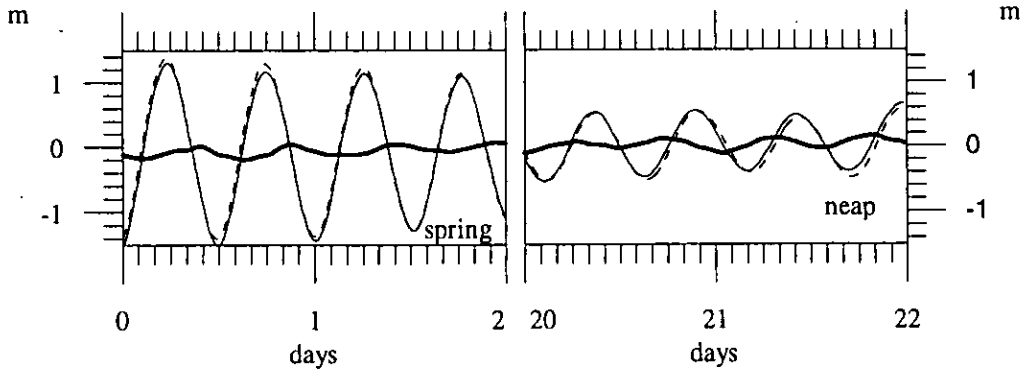

Fig. 9 *Sea level data from Stn E; original record (__) showing the deviation from the mean including results from harmonic analysis giving computed (--) and residual records (thick line). Day 0 is 9 April 1993, 0.00h local time.*

Currents

Velocities and directions for both stations are shown in Figs 10 a-b. The maximum current velocity observed during spring was 1.2 m/s (at Stn W) compared to 0.95 m/s at Stn E. During neap, maximum velocities were 0.4 and 0.5 m/s respectively. The main directions were, as mentioned, 32 °(225°) for Stn E and 51°(245°) for Stn W, which fits well with the channel orientation at the entrance of the bay. An asymmetry is seen on the western station. It needs an explanation. The velocities are 25-30% higher during flood but the differences are more clear during the later stage of the flood. The effect shows up as a shallow water tide in the harmonic analysis (Table 8, annex). However, this asymmetry seems to be a simple hydraulic effect, caused by the position of the current meter near the Baixo Ribeiro, a shallow reef just south of the current meter position. Thus, the asymmetry is not to be looked upon as part of a residual circulation (see also discussion on fluxes), but just as a topographic effect.

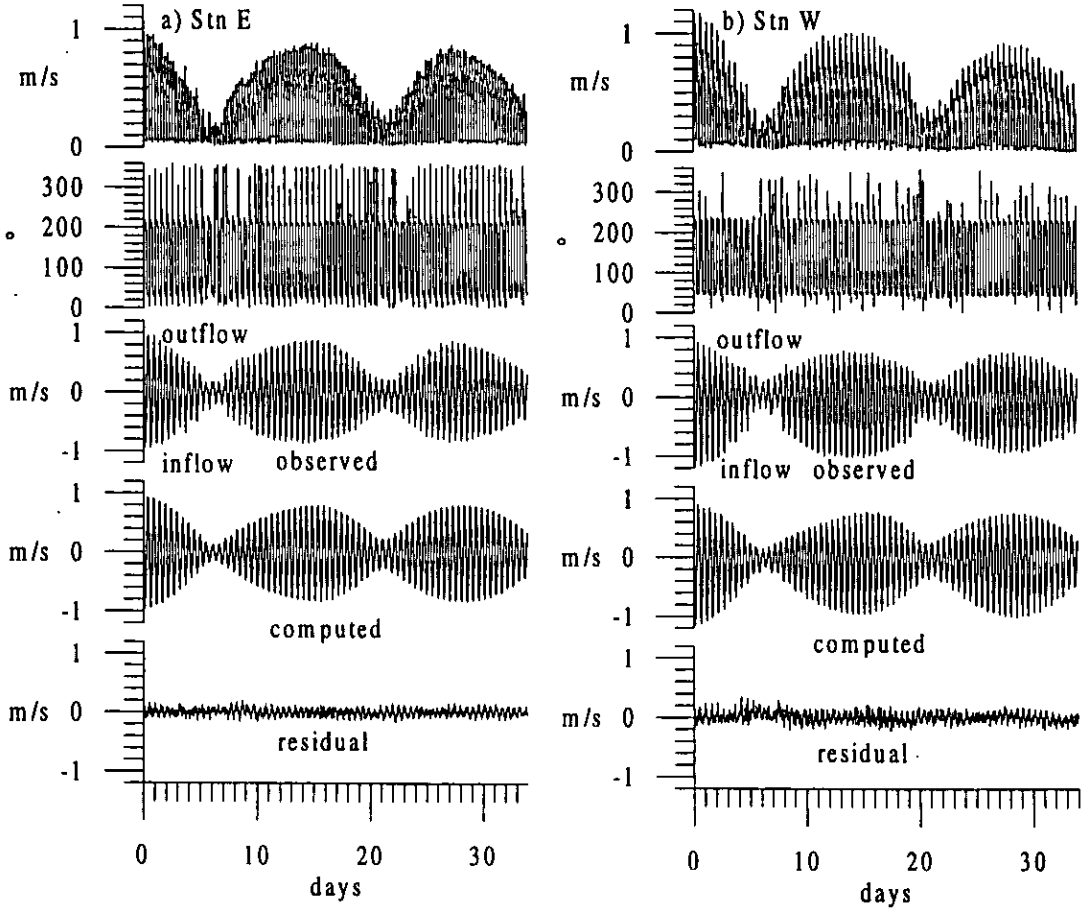

Fig. 10 a-b *Current meter data from Stn E at Ilha dos Portugueses and Stn W at Baixo Ribeiro showing current speed and direction including the velocity component along the direction of maxima variance 32° and 51° respectively and on it performed harmonic analysis (14 components; see text) giving computed and residual records. Day 0 is 9 April 1993 , 0.00 h, local time.*

Temperature

Original temperature records and those computed from harmonic analysis are shown in Figs 11 a-b and in Table 9. The temperature pattern indicates a decrease of about 2 °C (from 26.5 to 24.5) over whole period of 35 days, basically similar at both stations. The pronounced decrease in temperature is related to the normal seasonal change. A fortnightly cycle is also seen in the records. The short term variations are larger at spring than at neap, whereas the temperature shows more of a diurnal variation at stn W than at stn E. Stn W is situated near to the shallow part of the bay indicating that it is more sensitive to diurnal variations. Stn E on the hand has a larger semidiurnal signal with higher temperatures during outflow (not easily revealed from the figures). Higher temperatures during spring than during neap mirrors the more effective exchange (also the range increases). As mentioned before, however this is an effect of the season and during the southern summer, the temperatures are higher in the bay.

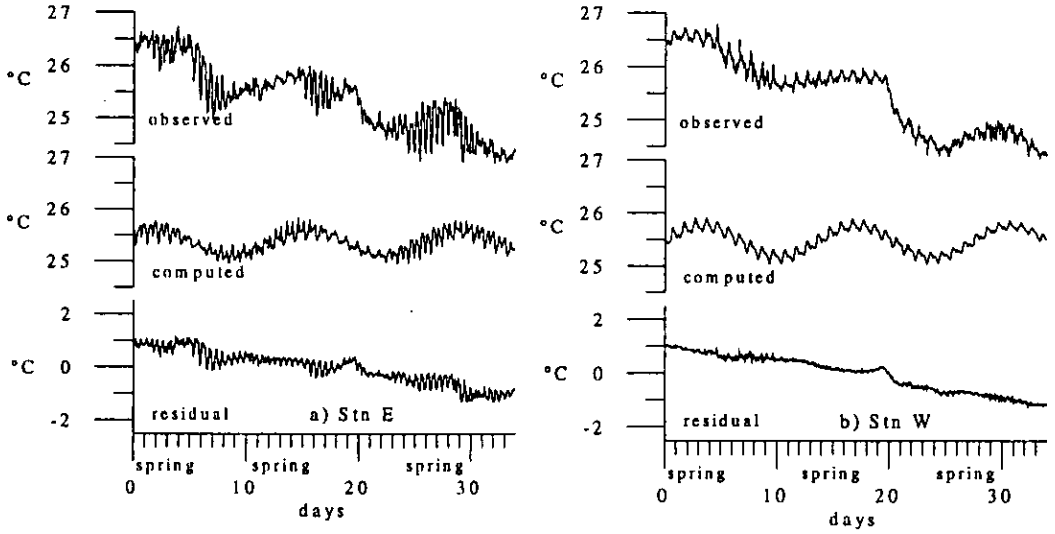

Fig. 11 *Temperature data from Stn E and Stn W including results from harmonic analysis giving computed and residual records. Day 0 is 9 April 1993, 0.00h, local time.*

Salinity

As for temperature also the salinity observations were subject to harmonic analysis. The results in terms of computed, observed and residual salinity are shown in Figs 12 a-b and in Table 10. At Stn E the salinity remained relatively constant during a long period but experienced a relatively rapid decrease of 2 psu after about 25 days. On Stn W, on the other hand a salinity decrease is seen already during the first neap period. The higher salinities, about 35.3 psu seen in the beginning of the period coincide with values typical for the Indian ocean waters. They were even some what higher compared to maximum salinities reported from this area (Saetre and da Silva, 1984). The lower salinities appearing in the end of period, indicate increasing freshwater

supply. Unfortunately there were only very sparse observations of discharge during this period (Fig. 8). Data on runoff and precipitation does not clearly indicate that such a strong decrease of the salinity would appear in the bay. This means that it is difficult to obtain results on water exchange from salt and volume balance, only.

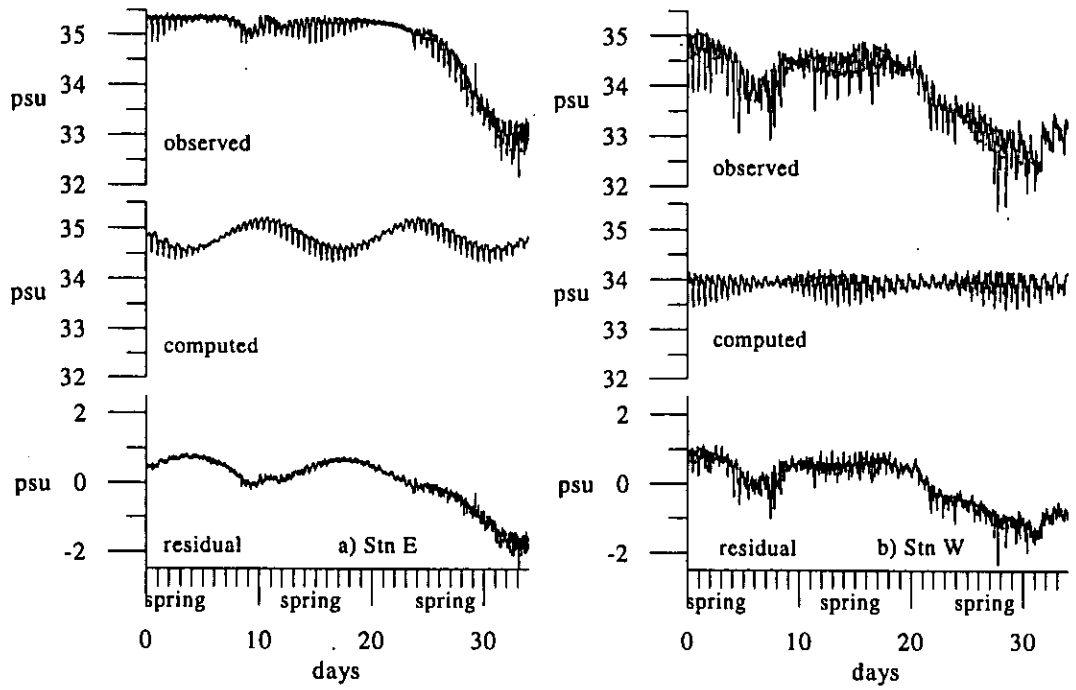

Fig. 12 *Salinity data from Stn E and Stn W including results from harmonic analysis giving computed and residual records. Day 0 is 9 April 1993, 0.00h, local time.*

There is also clear tidal influence on the short term salinity variations which is more easily seen from the two-day record shown in Figs 13 a-b. Partially the salinity variation follows the current pattern. At maximum ebb currents the salinity starts to decrease up towards minimum values occurring approximately at time of slack water. The correlation is not quite clear-cut, however, and different appearance may indicate not only an east-west salinity variation with lower salinities on the land-ward (western) side of the bay, but also effects of a vertical stratification which could appear on the western side where all rivers are entering the Maputo Bay. In the case of vertical stratification, the depth of halocline is of course important for the correlation between salinities and velocities.

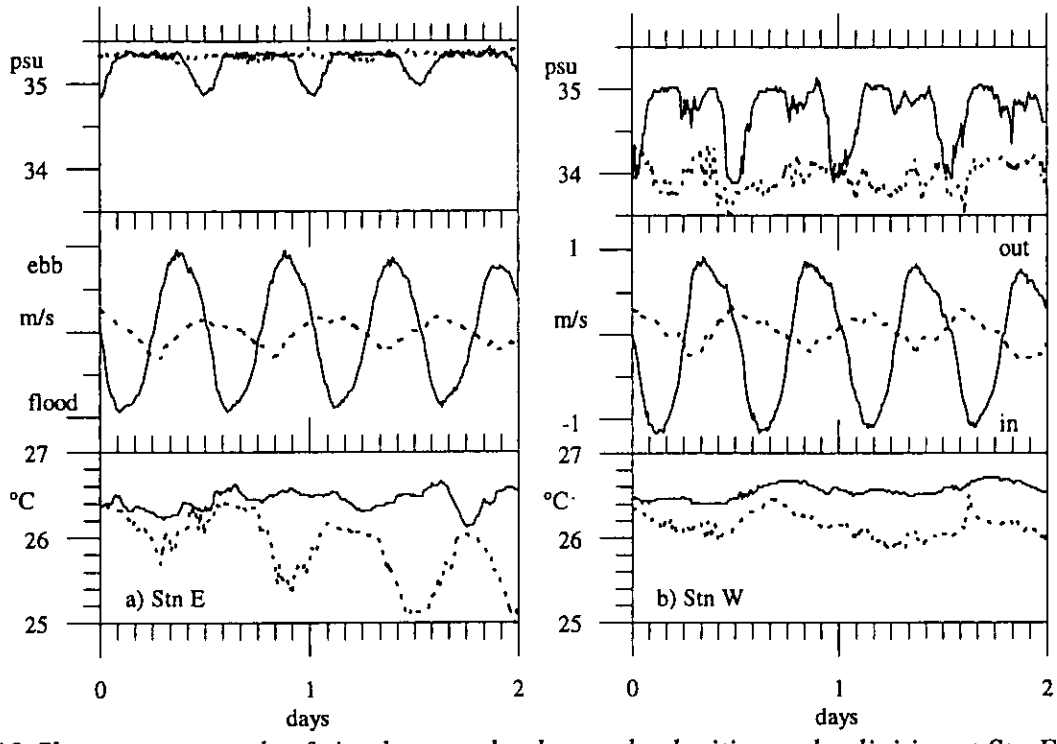

Fig. 13 *Short term records of simultaneously observed velocities and salinities at Stn E and W during 9 -10 April (___spring) and 15 -16 April (----neap) respectively. Start at 0.00h, local time.*

5.3 Computed fluxes

Figs 14 a-d show salt and volume fluxes calculated as $m(S)$, $m_s(S)$, $M(S)$ and $M_s(S)$ as described in Section 4.4. As seen from Fig. 14 d the total salt flux $M_s(S=S_{max})$ is zero, whereas a small net flux of water outwards is indicated from Fig.14 c. The main outflow takes place in the interval from 34.7-34.9 (approx. 3000 m^3/s; Fig.14 b), whereas the inflow occurs mainly at salinities from 34.9-35.1, here somewhat larger than 3000 m^3/s. For lower salinities, the flow is indifferent, representing a set of "events" with both in and outflows with approximately with equal salinities. However, a weak net outflow is indicated also for salinities lower than 34.7 (~500 m^3/s). The $M(S)$-curve does not end up at zero; in fact the deviation indicates the net fresh-water input to the bay. It's value is approx. 250 m^3/s. This value, however is by no means exact; mainly for the reason that we manipulated the velocities to obtain zero salt flux, a procedure which will also affect the $M(S_{max})$.

Clearly however, the exchange of water is dominated by net in- and outflows of approx. 3000 m^3/s in the interval from 34.7-35.2. This net flux, q_n , may be multiplied by a turbulent lengthscale l and divided by a cross-section area a to yield an exchange coefficient $u_l=q_n l/a \approx 500$ m^2/s. The residence time (e-folding) for the bay water vs ocean water is then $T_r=V/q_n \approx 14$ days.

Finally the freshwater supply q_f may be calculated from the equation $\partial(VS_b)/\partial t = q_n(S_o - S_b) - q_f S_b$, where VS_b is the bay water salt content, S_b the salinity of the water and S_o the salinity of ocean water. During the last 1-2 weeks, the bay water salinity decreased by 1-2 psu, i.e. ≈1psu/week. Assuming $S_b=34$ and $(S_o-S_b)=\Delta S=1$ yields $q_f \approx 250$ m^3/s. By coincidence, this very coarse estimate equals the figure for freshwater supply obtained in the M(S)-curve. Thus, the figures obtained are most likely the right order of magnitude (cf. Fig. 7), but as mentioned there is not enough data on the river flows for 1993 to compare with.

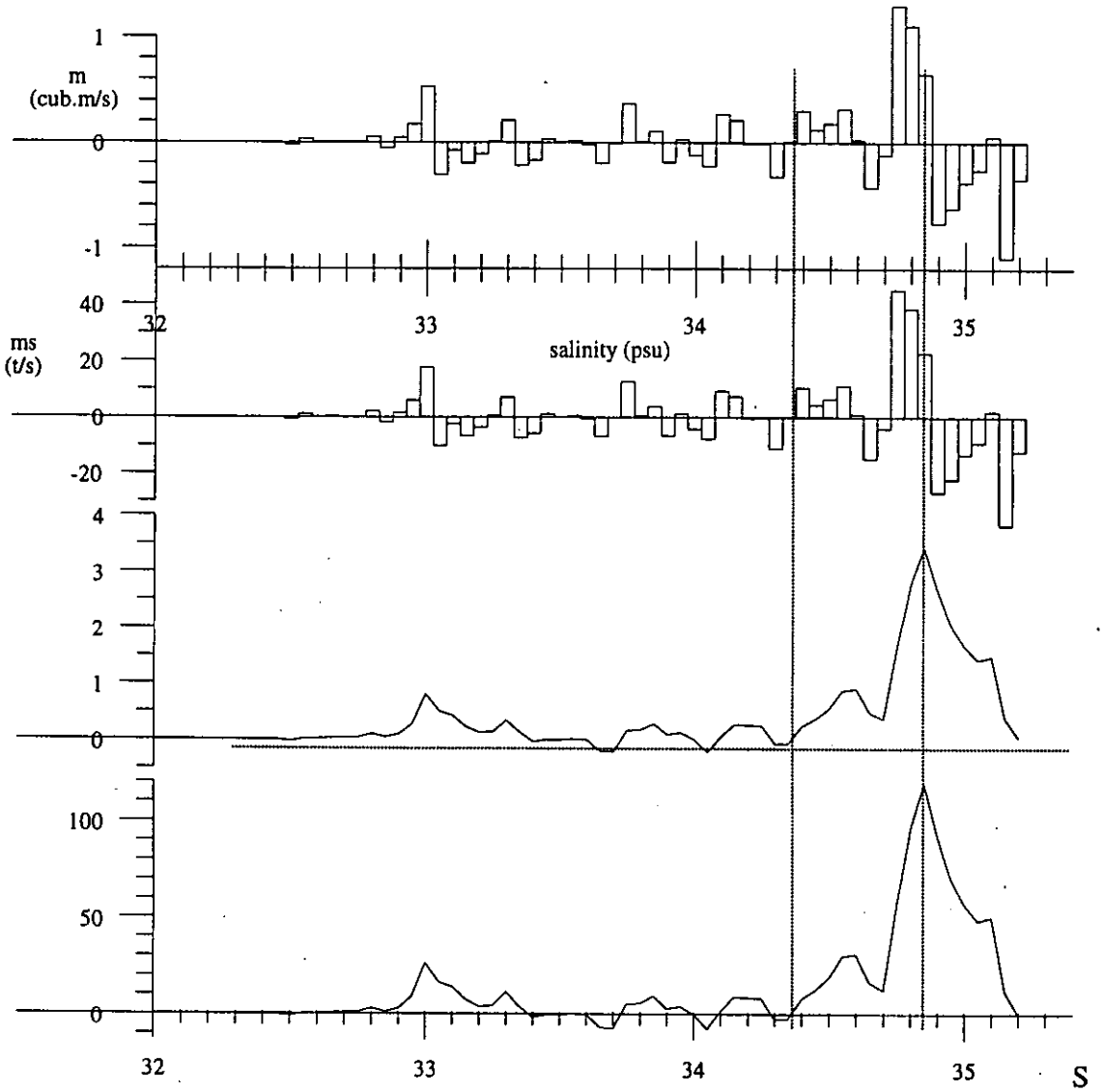

Fig. 14 *Volume and salt flux, (bars) instantaneous flux: a- m(S) in [$m^3/s*10^3$], b- $m_s(S)$ in [$kg/s*10^3$], c- integrated volume flux, M(S) in [$m^3/s*10^3$], and d- integrated salt flux $M_s(S)$ in [$kg/s*10^3$].*

As seen from Fig. 14a (*m(S)*), outflow occurs mainly for lower salinity while inflow occurs for higher. This indicates an inflow on the eastern side of the bay and an outflow on the western (see Figs 12 a-b and Figs 13 a-b, showing that salinity are lower on the western side). Comparing the

net flows, which are of the order of 3000 m^3/s, with the typical tidal flow 10^5 m^3/s it is obvious that any mean circulation in the bay is weak, a few cm/s at most. Postulating a weak clockwise circulation, however, contradicts the results from the current meter at stn W, which actually recorded higher in than outflows. As mentioned however, this RCM was situated behind a reef just inside of mooring, hindering the outflow to reach the current meter.

The heat flux is shown in Fig. 15. Maximum flux during inflow is approx. $25*10^9$ kW, corresponding to net flux (integrated over a half tidal cycle) of $60*10^9$ kWh. We see that there is a considerable outflow of heat (Fig 15 b) during the first neap period where the warmer water inside the bay (see Fig 11) is exported. Later the temperatures are becoming more similar and the heat flux variations are not that large. Over the period as a whole the flux is limited which is also expected as the temperatures inside and outside become more equal.

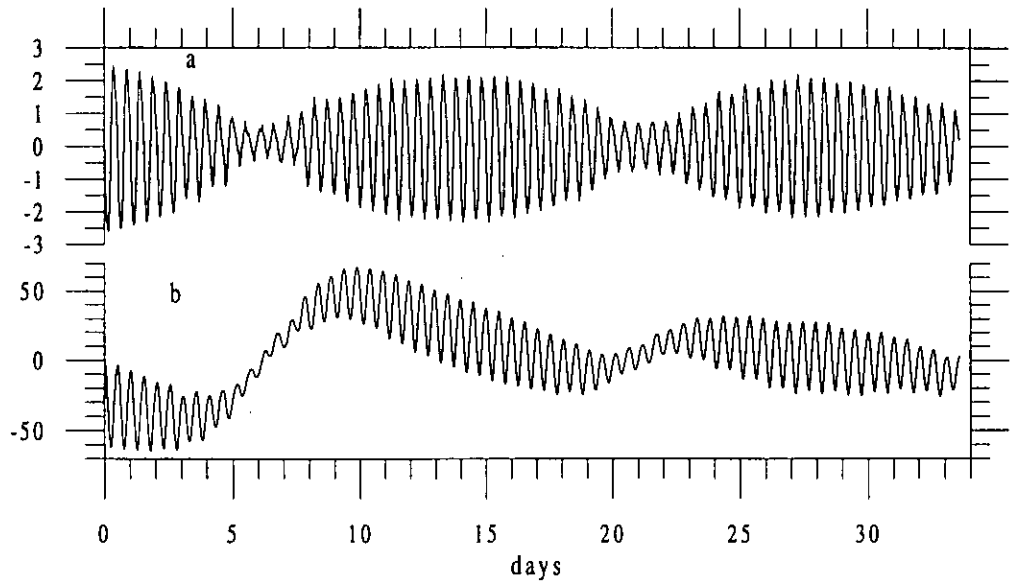

Fig. 15 Heat flux: a- instantaneous heat flux[kW10^{10}], b- integrated heat flux, defined such that minus is inwards [kWh*10^9]*

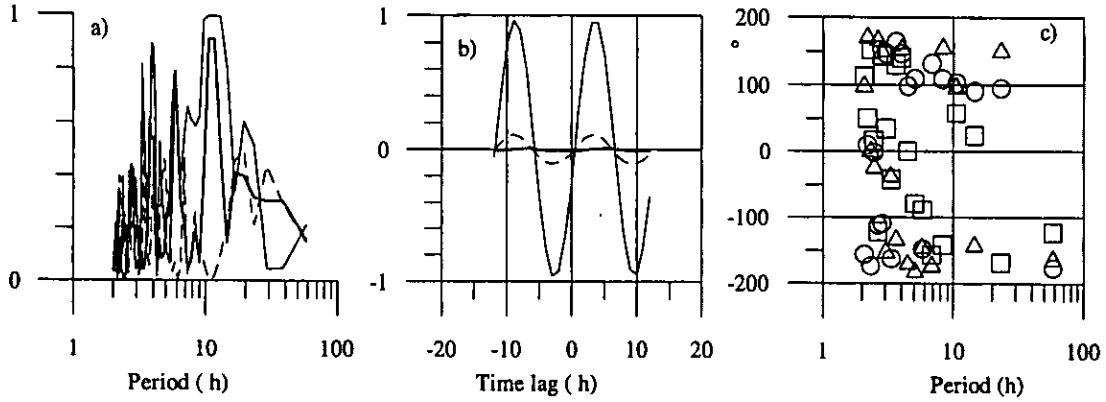

Fig. 16 *The cross-correlation analysis shown, a- coherence function, b-cross correlation function and c- phase lag between, salinity, velocity and temperature and elevation.*

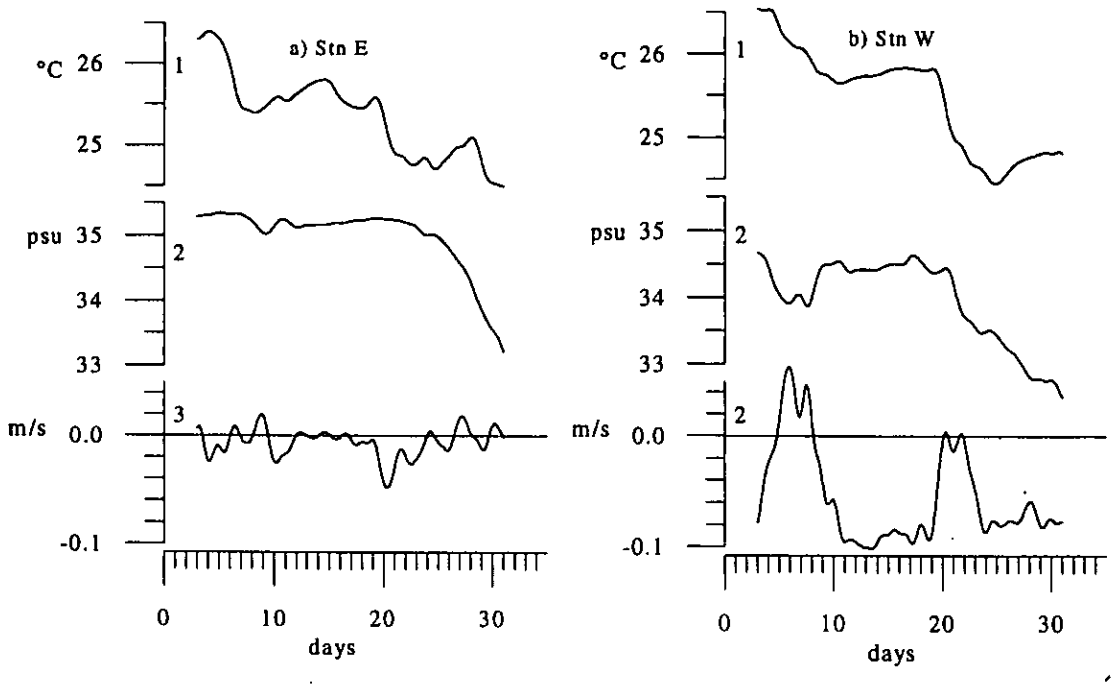

Fig. 17 *The low-pass filtered data for a) Stn E and b) Stn W: 1- temperature, 2- salinity and 3- current velocity*

The cross correlation between different parameters are shown in Figs 17 a-c. The salinity is less correlated with the temperature than with velocity and elevation. On average the parameters are more coherent for the M_2 constituent. At this point the phase lags are shown in the Fig.17 b, the maximum correlation is at 3h for salinity-velocity and salinity-temperature. The correlation functions show frequencies by which pairs of parameters are coherent. Thus, salinity and current are more coherent near to M_2 frequencies but not more than 0.9, followed by higher frequencies closer to S_4 and $2MS_6$. At a time lag of ±3h, salinity reaches its maximum correlation with the velocity (0.1) while at zero time lag there is no correlation at all.

6. CONCLUSIONS

Harmonic analysis showed that the tide is dominated by M_2. We found a spring tidal range of 2.5 m and a neap range of 0.7 m. The residence time for Maputo Bay water vs oceanic water is approx. 2 weeks. The corresponding long-term mean turbulent mixing coefficient κ_T is 500 m^2/s.

Although the current measurements showed a mean southward (i.e. inward flow) on Stn W, our interpretations of salinity data and salt/volume fluxes clearly indicate that there is a weak clockwise circulation of a few cm/s with outflow of lower salinities (river influenced) on the western side. It is reasonable to assume that this net flow is an effect of freshwater supply which was considerable during this period. Due to the coriolis force, the freshwater spreads more towards north along the coast, than towards east. However, as noted several times, this weak circulation is totally obscured in the current measurements which are dominated by a tidal circulation where the instantaneous velocities may reach 1 m/s or more. Even wind-generated velocities and flux may well exceed the residual fluxes.

7. ACKNOWLEDGEMENTS

I wish to express my deepest sense of gratitude to Lars Rydberg and Ulf Cederlöf, Department of Oceanography, University of Gothenburg, Sweden, for their guidance and inspiration during the period of study and their reviews of my manuscript, valuable comments and discussions. I am grateful to Noralf Slotsvik, Institute of Marine Research, Bergen, Norway, who provided the current meter and sea level data. This work has been studied under challenging discussions with Antonio Hoguane from Institute for Fisheries Research in Maputo and with Tor Gammelsröd from Geophysical Institute, University of Bergen. I am greatly indebted for their stimulating hints, discussions and encouragement. This work had not been successful without the good working environment in Physics Department at Eduardo Mondlane University and at the Department of Oceanography in Gothenburg, whose staff provided invaluable help.

The study was financially supported by the Swedish Agency for Research Corporation with developing countries, SAREC (Sida) through University of Gothenburg and by Universidade Eduardo Mondlane. Other institutions which collaborated were: Direcção Nacional de Águas, Instituto de Investigação Pesuqeira, Direcção Nacional de Aguas, Instituto Nacional de Meteorologia and Instituto Nacional de Hidrografia e Navegação.

8. REFERENCES

Arulananthan, K., Rydberg, L., Cederlöf, U. and Wijeratne, E. M. S. 1995. Water exchange in a hypersaline tropical estuary: the Puttalam Lagoon, Sri Lanka. *Ambio* **24**:438-443.

Andersson, L. and Rydberg, L. 1993. Exchange of water and nutrients between the Skagerrak and the Kattegat *Estuarine, Coastal and Shelf Science* **36**:159-181.

Bowden, K.F. 1983. Physical Oceanography of Coastal Waters. University of Liverpool. 302 pp.

Brown, W.S. and Trask, R. P. 1979. A study of tidal energy dissipation and bottom stress in an estuary. *Journal of Physical Oceanography* **10**:1742-1754.

Cederlöf U. 1998. *Msc lecture notes on Fluid Dynamics.* Department of Oceanography, University of Gothenburg.

Cheng, R.T and Gartner, J.W. 1985. Harmonic Analysis of Tides and Tidal Currents in South San Francisco Bay, California. *Estuarine, Coastal and Shelf Science* 21:57-74.

Doodson, A. T. 1921. The harmonic development of the tide generating potential. Proc. Roy. Soc, A. Vol. **100**: 305–329.

Donguy, J. R. and Piton, B. 1991. The circulation of Mozambique channel revisited. *Oceanologia Acta* **14**:549-558.

dos Muchangos, A. 1994. Cidade de Maputo: Aspectos geográficos, 93 pp

Dyer, K R. 1973. Estuaries: A physical Introduction. John Wiley & Sons, 140pp

Dyer, K R. and Taylor, P A. 1973. A simple segmented prism model of tidal mixing in well mixed estuaries. *Estuarine, Coastal and Marine Science* **1**:411-418.

Franco, A. S. 1981. Tides, Fundamental Analysis and Prediction 232 pp

Geyer, W.R. and Signell, P. R 1992. A reassessment of the role of tidal dispersion in estuaries and bays. *Estuaries* **15**:97-108.

Hoguane, A. M. 1994. Tidal currents and oil dispersion in Maputo Bay. Report, September 1994. IIP, Maputo, Mozambique

Hoguane, A M. 1996. Hydrodynamics, heat and salt budget in mangrove creeks and swamps. Ph. D Thesis. University of Wales, Bangor, UK.

Hughes, F.W. and Rattray, Jr. M. 1979. Salt Flux and Mixing in The Columbia River Estuary. *Estuarine, Coastal and Shelf Science* **10**:479-493

Iannielo, J.P. 1977. Tidally induced currents in estuaries of constant width and depth. *Journal of Marine Research* **35**:755-786.

Iannielo, J.P. 1981. Comments on tidally induced currents in estuaries : Dynamic and Near-Bottom flow characteristics f constant breath and depth. *Journal of Physical Oceanography* **11**:126-134

Henderschott, M. C. 1977. Numerical models of ocean tides. In "The Sea" (Goldberg et al., eds.) Vol. 6 pp. 47-95. Wiley. New York.

Henderschott, M. C. 1981. Long Waves and Oceanic Tides. In *Evolution of Physical Oceanography,* Ed. Bruce A. Warren and Carl Wunsch. MIT Press.1192-1341

Jay, A. J. and Smith, J. D. 1990. Residual circulation in shallow estuaries. 1. Highly stratified, narrow estuaries. *Journal of Geophysical Research* 95(C1):733-748

Jay, A.J. and Smith, J.D. 1990. Residual circulation in shallow estuaries. 2. Weakly stratified and partially mixed, narrow estuaries. *Journal of Geophysical Research* **95**:711-731

Lobo, M., Cunha, I. and Costa, M. 1973. Estudo da Oceanografia da Baia de Maputo. Relatório de investigaçao. DNA, Maputo

Medeiros, C. and Kjerfve, B. 1993. Hydrology of a tropical estuarrine system, Brazil. *Estuarine, Coastal and Shelf Science* **36**:495-515.

MINED. 1986. Atlas Geográficas de Moçambique.

Nestler, H., Pätsch, H-J. and Schmidt, W. 1984. Die Insel Inhaca und Entwicklung des Riffs vor Barreira vermelha. *Peters Geographishe Mitteilung* 1/84:31-37.

Oey, L Y. 1984. On steady salinity distribution and circulation in partially mixed and well mixed estuaries. *Journal of Physical Oceanography* **14**:629-645.

Officer, C. B. 1983. Physical oceanography of Estuaries and Associated Coastal Waters. John Wiley & Sons. 465 pp

Officer, C. B. and Kester, D. R. 1991. On estimating the non-advective tidal exchange and advective gravitational circulation exchange in an estuary. *Estuarine, Coastal and Shelf Science* **32**:99-103.

Pond, S. and Pickard, G. L. 1983. Introductory Dynamical Oceanography. 329 pp

Prego, R. and Fraga, F., 1992. A simple model to calculate the residual flows in a Spanish Ria - Hydrographic consequences in the Ria de Vigo. *Estuarine, Coastal and Shelf Science* **34**:603-615.

Queface, A. J. 1996. Temperature and salinity variability at the entrance of Maputo Bay. In Nansen Courses in Environmental Physics 95: Alte Brücke, Swakopmund, Namibia November 15-December 13 1995] Ed. by Tor Gammelsröd, Institute of Marine Research, Bergen, Norway

Robinson, I. S. 1983. A tidal flushing model of the fleet am English tidal lagoon
Estuarine, Coastal and Shelf Science 16:669-688.

Saide, F. V. 1996. Tidal Currents in Maputo Bay. In Nansen Courses in Environmental Physics 95: Alte Brücke, Swakopmund, Namibia November 15-December 13 1995] Ed. by Tor Gammelsröd, Institute of Marine Research, Bergen, Norway

Saetre, R.1985. The circulation of Mozambique channel. *Deep Sea Research* **32:**1457-67.

Saetre, R. and Jorge da Silva, A. 1984. The circulation of Mozambique channel. *Deep Sea Research* **31**:485-508.

Signell, P. R and Butman, B. Modeling Tidal exchange and dispersion in Boston Harbor. *Journal of Geophysical Research* **97**(C10):15591-15606.

Stigebrandt, A. 1980. Barotropic and baroclinic response of a semi–enclosed basin to barotropic forcing from the sea. *Fjord oceanography (eds. Lewings and Farmer).*

Swift, M. R. and Brown, W. S. 1983. Distribution of bottom stress and tidal energy dissipation in a well-mixed Estuary. *Estuarine, Coastal and Shelf Science* **17**:297-317.

Walin, G. 1977. A theoretical framework for the description of estuaries. *Tellus* **29**:128-136.

Wattayakorn, G., Wolanski, E. and Kjerfve, B. 1990. Mixing, trapping and outwelling in the Klong Ngao mangrove swamp, Thailand. *Estuarine, Coastal and Shelf Science* **31**:667-688.

Wong, K C. 1994. On the nature of transverse variability in coastal plain estuary. *Journal of Geophysical Research* **99**(C7):14209-14222.

9. TABLES

Name	Position		HWS	HWN	LWS	LWN
	Latitude	Longitude				
Maputo harbour	25° 55' S	32° 34' E	3.5	2.4	0.5	1.6
Baixo Ribeiro	25° 55' S	32° 48' E	3.2	2.3	0.8	1.7
Baixo da Inhaca	25° 54' S	32° 55' E				

Table 1: *Height of tides from hydrographic reference level; for the Maputo harbour and Baixo Ribeiro, the entrance of Maputo Bay, from hydrographic Maps 46659-M, 1985; 496 A, 1995*

	T	*P*	*E*	*Ws*	*Wd (%)*								
	(°C)	*(mm)*	*(mm)*	*(m/s)*	*C*	*N*	*NE*	*E*	*SE*	*S*	*SW*	*W*	*NW*
Jan	26	157	107	3	0	3	15	58	3	13	7	0	0
Feb	26.9	137	93	2.9	0	1	9	46	1	30	12	0	0
March	25.3	97	97	2.5	0	0	16	51	0	21	12	0	0
April	23.7	58	88	2.5	0	9	24	28	0	24	13	0	0
May	21.8	38	92	2.6	0	16	16	13	0	22	25	0	4
Jun	19.5	19	87	2.5	0	16	24	12	0	15	25	0	4
July	19.2	18	92	2.6	0	19	22	22	0	18	16	0	1
August	20.3	15	145	3	0	21	33	27	0	13	6	0	0
September	21.5	48	100	3.2	0	4	27	34	3	22	9	0	0
October	22.5	55	101	3.2	0	3	31	42	0	18	6	0	0
November	23.7	80	97	3.0	0	6	24	34	3	24	7	0	1
December	25.2	91	207	3.1	0	10	15	57	1	10	4	0	0
Year	22.9	809	1163	2.8	0	9	21	35	1	19	12	0	1

Table 2 : *Meteorological data on air temperature T, precipitation P, evaporation E, wind speed Ws and direction Wd . Monthly mean figures from "Observatório de Maputo", INAM, for the period 1951-1990.*

	Incomati		Maputo		Umbeluzi	
	R (m^3/s)	P (mm)	R (m^3/s)	P (mm)	R (m^3/s)	P (mm)
Jan	156.6	100	145.8	110.7	75.7	117.6
Feb	262.7	126.7	234.5	97.6	125.9	113.6
March	172.1	91.1	162.3	57	75.9	75
April	99.2	39.8	92.4	46.6	43.7	47
May	60.6	28.1	56.2	20.5	27	28.3
Jun	40.3	19.6	38.8	14.5	18.1	14.6
July	29.3	16.3	42.1	20.3	13.5	14.1
August	21.8	25.1	26.3	11.8	13.4	12.2
September	17.6	31.2	24.5	32.1	12	34.1
October	33.5	42.5	42.9	51.1	24.6	53.5
November	45.9	47.4	80	69.7	34.6	70.8
December	112.4	81	135.6	74.2	61.3	87.6
Year	87.7	648.5	90.1	606.2	43.8	688.4

Table 3 : *Long-term data on runoff R and precipitation P for the period 1951-1990 (from DNA and INAM).*

Rivers	Present Runoff (km^3/year)	Saetre and da Silva 1984 (km^3/year)	Ataíde 1981 (m^3/year)
Incomati	2.8	2.4	3.9
Umbeluzi	1.4	-	-
Maputo	2.8	2.9	-
Total	7	5.3	

Table 4 : *River runoff for the main rivers precipitation P, during 1993(data from INAM).*

Instrument type	Station	Parameter	Accuracy
Current meter Aanderaa RCM-7 10609	W	Current speed Current direction Temperature Conductivity Pressure	1 cm/s 5 ° 0.05 °C 0.1 m/cm 0.5 %
Currentmeter RCM-7 10976	E	(dito)	(dito)
Tide gauge Aanderaa WL 476	E	Pressure Temperature	0.5%

Table 5 : *Characteristics of the instrument; types and accuracy of the sensors.*

Parameter	*Formula*	*Interpretation*	*Maputo Bay*
Form number	$(K_1+O_1)/(M_2+S_2)$	Semidiurnal tide	0.06
Phase Inequality Relationship	$M_2°-(K_1°+O_1°)$	Diurnal inequality predominatly in high waterss	-104.3 h (-5.3 d)
Phase Age	$0.98(S_2°-M2°)$	Time that spring tide occurs after new or full Moon	38.8 h (1.6 d)
Mean range	$2.2(M_2)$	Average tidal range (semidurnal)	1.78 m
Spring range	$2.0(M_2+S_2)$	Average range during spring tide (semidurnal and diurnal	2.52 m
Neap range	$2.0(M_2-S_2)$	Average range during neap tide (semidurnal)	0.72 m
Tropic range	$2.0(K_1+O_1)$	Average range during tropic tide (diurnal)	0.16 m
Equatorial range	$2.0(K_1-O_1)$	Average range during equatorial tide	0.04 m
Diurnal Age	$0.91(K_1°-O_1°)$	Time that tropic tide occurs after maximum semi montlhy declination of the Moon.	163 h (7 d)

Table 7: *Tidal statistics based on the harmonic constituents in Maputo Bay (9 April - 13 May 1993)*

Constituents		Station E		Station W	
Symbol	*Period (hours)*	*Amplitude (m/s)*	*Phase (°)*	*Amplitude (m/s)*	*Phase (°)*
Mf	327.8689	0.01	163.5	0.04	327.7
K_1	23.9344	0.001	133.6	0.03	231.1
O_1	25.8194	0.01	100.0	0.01	143.5
P_1	24.0659	0.01	320.0	0.01	10.17
M_2	12.4206	0.53	189.7	0.56	191.1
S_2	12.0000	0.32	239.3	0.31	243.2
N_2	12.6584	0.07	168.4	0.07	163.3
K_2	11.9672	0.14	222.7	0.15	232.0
$2SM_2$	11.6070	0.03	31.2	0.03	17.9
M_4	6.2103	0.01	131.2	0.05	216.6
MS_4	6.1033	0.003	53.6	0.06	261.6
S_4	6.0000	0.003	181.5	0.02	349.1
M_6	4.1402	0.02	25.6	0.02	33.4
$2MS_6$	4.0924	0.03	72.7	0.04	49.7

Table 8: *Results of harmonic analysis of elevation and current velocity at stations E and W*

Constituents		Station E		Station W	
Symbol	*Period (hours)*	*Amplitude (°C)*	*Phase (°)*	*Amplitue (°C)*	*Phase (°)*
Mf	327.8689	0.26	190	0.32	232.2
K_1	23.9344	0.03	55.6	0.06	359.3
O_1	25.8194	0.01	77.9	0.01	316.5
P_1	24.0659	0.04	159.8	0.06	191.7
M_2	12.4206	0.01	225.3	0.02	123.1
S_2	12.0000	0.11	356.7	0.01	89.7
N_2	12.6584	0.04	96.5	0.002	287.8
K_2	11.9672	0.1	238.5	0.03	139.6
$2SM_2$	11.6070	0.08	37.6	0.01	204.7
M_4	6.2103	0.01	347.2	0.01	19.2
MS_4	6.1033	0.03	358.3	0.01	55.2
S_4	6.0000	0.04	343.9	0.003	135.4
M_6	4.1402	0.01	236	0.003	308.7
$2MS_6$	4.0924	0.01	281.2	0.01	267.9

Table 9: *Results of harmonic analysis of temperature at Stn E and W*

Constituents		Station E		Station W	
Symbol	*Period (hours)*	*Amplitude (psu)*	*Phase (°)*	*Amplitue (psu)*	*Phase (°)*
Mf	327.8689	0.29	54.2	0.03	17
K_1	23.9344	0.08	303.7	0.1	156
O_1	25.8194	0.01	91.2	0.02	66.8
P_1	24.0659	0.09	233	0.08	126.3
M_2	12.4206	0.08	104.2	0.1	85.1
S_2	12.0000	0.05	151.1	0.07	239.1
N_2	12.6584	0.02	90.9	0.04	11.1
K_2	11.9672	0.03	151.3	0.09	174.4
$2SM_2$	11.6070	0.01	250.7	0.01	160.4
M_4	6.2103	0.04	335.3	0.09	22.3
MS_4	6.1033	0.05	21.3	0.1	55.3
S_4	6.0000	0.01	14.5	0.03	33.5
M_6	4.1402	0.01	228.3	0.03	262.5
$2MS_6$	4.0924	0.01	258.3	0.03	259

Table 10: *Results of harmonic analysis of salinity at Stn E and W*